

Proceedings of the ASME 2020 Conference on Smart Materials,
Adaptive Structures and Intelligent Systems
SMASIS2020
September 15, 2020, Virtual, Online

# **SMASIS2020-2390**

# A COMPUTATIONAL FRAMEWORK FOR PREDICTING PROPERTIES FROM MULTIFIELD PROCESSING CONDITIONS IN POLYMER MATRIX COMPOSITES

Denise Widdowson, and Paris von Lockette The Pennsylvania State University, State College, PA

Anil Erol Materials and Manufacturing Directorate, The Air Force Research Laboratory, Wright-Patterson, OH

Manuel A. Rodriguez University of Maryland

## **ABSTRACT**

Composites can be tailored to specific applications by adjusting process variables. These variables include those related to composition, such as volume fraction of the constituents and those associated with processing methods, methods that can affect composite topology. In the case of particle matrix composites, orientation of the inclusions affects the resulting composite properties, particularly so in instances where the particles can be oriented and arranged into structures. In this work, we study the effects of coupled electric and magnetic field processing with externally applied fields on those structures, and consequently on the resulting material properties that arise. The ability to vary these processing conditions with the goal of generating microstructures that yield target material properties adds an additional level of control to the design of composite material properties. Moreover, while analytical models allow for the prediction of resulting composite properties from constituents and composite topology, these models do not build upward from process variables to make these predictions.

This work couples simulation of the formation of microscale architectures, which result from coupled electric and magnetic field processing of particulate filled polymer matrix composites, with finite element analysis of those structures to provide a direct

Keywords: magneto-active elastomer; smart materials; materials processing; non-equilibrium processing; polymer matrix composites;

ASME disclaims all interest in the U.S. Government's contribution.

#### **NOMENCLATURE**

Re|K|: degree of polarization.

 $\omega$ : AC field frequency.

τMW: Maxwell-Wagner charge relaxation time.

v: Poisson's Ratio.

D: Compliance Matrix

*N*: Number of particles.

 $\mathbf{E}_0$ : External magnetic field.

and explicit linkages between process, structure, and properties. This work demonstrates the utility of these method as a tool for determining composite properties from constituent and processing parameters. Initial particle dynamics simulation incorporating electromagnetic responses between particles and between the particles and the applied fields, including dielectrophoresis, are used stochastically generate representative volume elements for a given set of process variables. Next, these RVEs are analyzed as periodic structures using FEA yielding bulk material properties. The results are shown to converge for simulation size and discretization, validating the RVE as an appropriate representation of the composite volume. Calculated material properties are compared to traditional effective medium theory models. Simulations allow for mapping of composite properties with respect to not only composition, but also fundamentally from processing simulations that yield varying particle configurations, a step not present in traditional or more modern effective medium theories such as the Halpin Tsai or doubleinclusion theories.

**x**: Position vector.

d: Orientation of semi-minor axis unit vector.

M: Particle magnetization strength.

R: Particle radius.

*V*: Particle volume.

 $\mathbf{F}_k$ : k-type force acting on a particle.  $\mathbf{T}_k$ : k-type torque acting on a particle.

 $\epsilon_0$  : Permittivity of free space

This work was authored in part by a U.S. Government employee in the scope of his/her employment.

 $\epsilon_p$ : Permittivity of a particle

 $\epsilon_0$ : Permittivity of the matrix.

 $\mathbf{r}_i$ : Vector pointing from particles i to n.

 $\hat{\mathbf{r}}_i$ : Unit vector of  $\mathbf{r}_i$ .

Q: Scaling parameter for repulsive force

D: Drag coefficient.

 $\eta$ : Dynamic viscosity.

ω: Angular velocity.

m: Particle mass.

*J*: Particle moment of inertia.

Λ: side length of unit cube RVE

 $\epsilon_{i,j}$ : the I,j component of small strain

 $\sigma_{i,j}$ : i,j component of the nominal stress

#### 1. INTRODUCTION

Exploration of processing – structure- property is a key area of study in material science. Traditional effective medium theory is a powerful tool for determining the material properties of various composites from those underlying structures. Several theories have been developed over time, such as the Halpin-Tsai model and the Mori-Tanaka model, both of which are widely used with various composites [1]–[3]. However, as these models use only parameters pertaining to composition, or nominal metrics of structure, they do not directly take into account the effects of processing parameters, specifically how the structures are formed by the processing. Precisely controlling microstructures during processing is a crucial mechanism for manipulating the properties of composite materials. Material systems consisting of filler material embedded in a matrix can be structurally modified to change several bulk properties, including those related to mechanical, magnetic, and electric responses[4]-[7].

In this work, initial particle dynamics simulations, ultimately coupled with finite element methods, are used to bridge the complex predictive gap between processing and properties in an electro-magnetically processed polymer matrix The work is motivated by the use of electromagnetic field processing by researchers and those industry. For example, it is known that application of a static magnetic field on a ferrofluid, which is a colloidal suspension of ferromagnetic particles in a carrier fluid, will result in a change in the internal structure [8]. These particle-particle interactions manifest in observable surface instabilities, such as the Rosensweig effect [9], or a change in viscosity, known as the magnetoviscous effect [10], [11]. Studies have also reported that colloids embedded in a polymeric matrix can be manipulated to form chains with electric and magnetic fields [12]. Furthermore, recent studies have reported that a combination of magnetic and electric fields during the curing process of composites can arrange particles in multiple dimensions [13], and potentially create a hierarchy of structure where chains can contain smaller-scale structures whose primary axes do not align with the chain's axis [14].

These latter works involving coupled fields utilize dielectrophoresis. Dielectrophoresis describes the translation that is caused by an electric field due to induced dipoles, leading to unidirectional alignment of the particles within the colloid [13]. Although colloidal suspensions will respond readily to an AC or DC field, a DC field will result in electrophoresis, where charged particles move toward the oppositely charged electrode [12]. An AC electric field however can result in a net electrostatic force, due to dielectrophoresis, which causes particle motion [15]. The benefit of using an AC field is the potential for precise motion control via manipulation of parameters such as field strength and frequency [12]. The frequency of an applied field, conductance of the particles and the medium; particle size, particle shape, and particle number ratio can be used to tune structures formed in a biparticle colloidal system [16]. The dielectrophoretic mechanism that directs particle micro architecture formation results directly from the particles' electric dipole vectors whose direction lies along their polarization axis. and whose polarization strength can be described using the Clausius-Mossotti function [17].

$$Re|K| = \frac{\varepsilon_2 - \varepsilon_1}{\varepsilon_2 + 2\varepsilon_1} + \frac{3(\varepsilon_1 \sigma_2 - |\varepsilon_2 \sigma_1)}{\tau_{MW}(\sigma_2 + 2\sigma_1)^2(1 + \omega^2 \tau_{MW}^2)}$$
(1)

where Re|K| shows the degree of polarization,  $\epsilon_1$  and  $\sigma_1$  are the dielectric permittivity and conductivity of the media,  $\epsilon_2$  and  $\sigma_2$  are the dielectric permittivity and conductivity of the particles,  $\omega$  is the AC field frequency, and  $\tau$ MW is the Maxwell–Wagner charge relaxation time defined by

$$\tau_{MW} = \frac{\varepsilon_2 + 2\varepsilon_1}{\sigma_2 + 2\sigma_1} \tag{2}$$

Dipoles induced in particles in a proximity of one another interact and align to form chains, driven by the field strength squared and the radius of the particle squared. Particles of the same type always align along field lines regardless of the media of the colloid [17]. Simultaneously, external magnetic and AC electric fields acting on particles can be tuned to control the structures and networks formed. Particles can be coerced into forming directional chains or 2D networks with various field configurations. The resulting properties of the composite, such as mechanical, thermal, and dielectric, containing such particle structures depend on the configuration of the particles [13].

In the work herein, the simulations are meant to model the response of barium hexaferrite, and ferromagnetic particle with a hexagonal plate-like geometry. From SEM studies, we have observed that the particles have thickness of  $\sim\!\!1~\mu m$ , and median hydraulic diameter of  $\sim\!\!7\mu m$ . Consequently, Brownian motion is not considered dominant. This argument for particles of this size is supported by other researchers [8].

Additionally, while the polymer fluid at first fully liquid, the fluid is cured with addition of heat while still under the influence of the external fields. Consequently, structures produced are fixed in place during curing. This process is meant to model the curing behavior of Dow Corning Sylgard elastomer compound.

Finite element analysis of these particle structures' resulting material properties have been found to correlate well to effective medium theory, such as the Mori-Tanaka model [18], [19]. Finite element analysis estimation of material properties is most efficiently done through the use of a representative volume element (RVE) due to the computational cost of large simulations. Of particular concern with such simulations is the size of the volume used. If the simulation is overly simplified the results will be inaccurate, while larger models use significant resources to solve. A convergence study on physical properties can be used to determine the appropriate size of a model, such as was done by Pahlavanpour et al. [20], where the effective modulus was used to determine convergence. It was determined that for large discrepancies in modulus between the matrix and the particles, that larger RVE's were required for accurate results. In [20] it was shown that the minimum RVE size required for convergence is 5% larger when the modulus discrepancy between particle and matrix modulus is increased from approximately 9.5 to 13 times greater.

The overarching goal of this work is to predict effective properties of polymer matrix composites whose micro architectures result from electromagnetic processing. The work uses existing simulation software, developed by the authors, to predict those architectures for proscribed processing conditions on a proscribed constituent set. Next, this work develops new software tools that take tabulated data from processing simulations, generates solid (CAD) models, and subsequently analyzes those models using COMSOL Multiphysics, a commercial finite element software package. Consequently, this document reports results of simulations and property estimations undertaken to assess the method's ability to converge to a representative volume element and subsequently to accurately predict effective moduli. Accuracy of predicted moduli is made by comparison to existing validated effective medium theories.

#### 2. MATERIALS AND METHODS

In this work, N ellipsoidal particles are assumed distributed in a polymer matrix of volume V and subjected to an applied electric field vector  $E_0$ . Particle positions, x, and orientations, d, are determined for a selected set of processing parameters following the simulation of particle dynamics driven by classical electromechanics.

#### Governing forces

The dynamics of colloidal suspensions of electromagnetically susceptible particles are governed by several types of interactions including thermal, diffusive, electromagnetic and hydrodynamic. For micrometer sized particles, diffusion and thermal motion can be safely neglected [21]–[24]. The governing forces under this assumption are then electromagnetic, hydrodynamic and contact forces; gravity is neglected due to the colloidal assumption.

## *Hydrodynamic forces and torques*

As observed in the literature, the Reynolds number associated with the motion of a particle acted on by external fields in similar suspensions is on the order of  $10^{-6}$  [24]–[26]. We can, therefore, model hydrodynamic forces as Stoke's Drag. The force that the fluid exerts on particle n as it tries to translate is then given by:

$$\left(\mathbf{F}_{drag}\right)_{i} = -D\dot{\mathbf{x}}_{i} \tag{3}$$

where D is the drag coefficient. Assuming a spherical particle of hydraulic radius R in a fluid with dynamic viscosity  $\eta$ , drag is given by  $D = 6\pi\eta R$ .

Particles also experience resistance to rotational motion. This hydrodynamic torque can be modeled by:

$$\left(\mathbf{T}_{drag}\right)_{i} = 8\pi\eta R^{3}\mathbf{\omega}_{i} \tag{4}$$

where  $\omega_n$  is the angular velocity of particle n, which can be defined in terms of the particle orientation  $\mathbf{d}_i$  by:  $\omega_i = \mathbf{d}_i \times \dot{\mathbf{d}}_i$ .

# Repulsive forces

Traditional models for hard sphere interactions are employed in numeric simulations to produce repulsive forces [25]–[27]

$$\left(\mathbf{F}_{rep}\right)_{i} = \sum_{j=1}^{N} Q * e^{-\beta(\frac{r_{m}}{2R}-1)} \,\hat{\mathbf{r}}_{j} \tag{5}$$

where Q is a variable scaling factor adjusted to ensure stability of the simulations, and  $r_j$  is the position vector between particles i and j.

#### Electromagnetic forces and torques

The particles are also assumed to have a dielectric response, which yields dielectric forces and torques. The dielectrophoretic force experienced by particle i is

$$(\mathbf{F}_{dep})_i = (\mathbf{p}_i \cdot \nabla) \mathbf{E}_i, \tag{6}$$

where  $E_i$ , is the sum of the external field and all field contributions of other particles, computed at the  $i^{th}$  particle's location.

The dielectrophoretic torque on the  $i^{th}$  particle is given by

$$\left(T_{dep}\right)_{i} = p_{i} \times E_{i} \tag{7}$$

where the polarization of particle i,  $p_i$ , is computed from

$$p_{i} = V_{p} \left(\varepsilon_{p} - \varepsilon_{m}\right) \left(\frac{E_{0} \cdot \hat{e}_{i}^{1}}{1 + \left(\frac{\varepsilon_{p} - \varepsilon_{m}}{\varepsilon_{m}}\right) L_{1}} \hat{e}_{i}^{1} + \frac{E_{0} \cdot \hat{e}_{i}^{2}}{1 + \left(\frac{\varepsilon_{p} - \varepsilon_{m}}{\varepsilon_{m}}\right) L_{2}} \hat{e}_{i}^{2} + \frac{E_{0} \cdot \hat{e}_{i}^{3}}{1 + \left(\frac{\varepsilon_{p} - \varepsilon_{m}}{\varepsilon_{m}}\right) L_{3}} \hat{e}_{i}^{3}\right)$$

$$(8)$$

where  $V_p$  is the particle volume  $\epsilon_p$  and  $\epsilon_m$ , are the permittivities of a particle and the matrix, respectively. Note also that  $L_i$  are the depolarization factors of an elliptical particle with respect to an orthonormal basis  $\hat{\boldsymbol{e}}_1 - \hat{\boldsymbol{e}}_2 - \hat{\boldsymbol{e}}_3$ .

The particles are also assumed to be acted on by magnetic forces and torques. The magnetic force is given by

$$(\mathbf{F}_{mag})_{i} = -\mu_{0} M V_{p} \nabla (\mathbf{H}_{i} \cdot \boldsymbol{d}_{i})$$
(9)

and the torque by

$$\left(\mathbf{T}_{mag}\right)_{i} = \mu_{0} M V_{p}(\mathbf{d}_{i} \times \mathbf{H}_{i}) \tag{10}$$

where  $H_i$  is the sum, at the location of the  $i^{th}$  particle, of the stray fields given off by all particles.

# **Equations of motions**

The forces acting on particle i determine the evolution of its state variables  $\mathbf{x}_i$  and  $\mathbf{d}_i$  by Newton's second Law. The equations of motion for the i<sup>th</sup> particle are then:

$$m_i \ddot{\mathbf{x}}_i = \left(\mathbf{F}_{mag}\right)_i + \left(\mathbf{F}_{dep}\right)_i + \left(\mathbf{F}_{drag}\right)_i + \left(\mathbf{F}_{rep}\right)_i \tag{11}$$

and

$$J_{i}(\mathbf{d}_{i} \times \ddot{\mathbf{d}}_{i}) = (\mathbf{T}_{mag})_{i} + (\mathbf{T}_{dep})_{i} + (\mathbf{T}_{drag})_{i}$$
(12)

where  $m_i$  and  $J_i$  are the mass and moment of inertia of particle i.

The particles are assumed to exist in a representative cubic volume element with side length  $\Lambda$  that is computed to yield to appropriate volume fraction f,

$$\Lambda = \left(\frac{4\pi R^3 N}{3f}\right)^{\frac{1}{3}} \tag{13}$$

Processing Simulation Boundary conditions

We defined a representative volume element (RVE) containing a finite number of particles to represent the behavior of the system away from the fluid surface. Also, we used three dimensional nearest neighbor periodic boundaries on the RVE, e.g. a particle that exits the boundary returns on its mirrored boundary at the corresponding exit point with the same velocity,  $\dot{x}$ . Details of methods of temporal discretization, specific numerical schemes employed, and error estimation may be found in [24].

#### 3. RESULTS OF SIMULATIONS AND ANALYSES

We can translated the numerical scheme developed in the previous chapter into a computational algorithm using Matlab®. To produce useful predictions from this simulation we need to select appropriate values for our governing constants, define quantitative parameters that characterize the observed structures, and determine the sensitivity of our code to the boundary and initial conditions.

# Simulation parameters

Our objective was to predict the micro-structure of MAE samples fabricated under two conditions, with and without an aligning electric field. We focus specifically on MAEs made of a polydimethylsiloxane (PDMS) matrix reinforced with barium hexaferrite particles. With this in mind we select fluid and particle characteristics that closely match the fabrication process of this material used by the authors in experiments [14].

- Particle volume fraction: f = 0.1
- Dynamic viscosity  $\eta$ : 3.5  $Pa \cdot s$
- Particle radius  $R: 0.5 \times 10^{-6} m$
- Particle magnetization M: 380 kA/m

For electric-field aligned cases, these simulations were performed under an excessively high unidirectional electric field, with amplitude of  $|||E_0||| = 100 \, MV/m$ , to simulate an electric field dominated system. For cases with no electric field alignment,  $E_0 = \mathbf{0} V/m$ . The external magnetic field in all cases was set to  $H_0 = 50 \, kA/m$  in simulations. This magnetic field strength is nominally low, equivalent to a refrigerator magnet, and is used because it reduces computational time without affecting chain alignment (See Figure 1a). The details of the reduction in computational time stem from the time integration scheme chosen as well as the determination of the repulsive force scaling factor, Q. The details can be found in Ref. [24]. This low magnetic field does not affect alignment because it is only 13.1% of the magnetization of the particles and is therefore energetically dominated by particle magnetization. Additionally, the electric field magnitude is assumed static, e.g. producing DC field. The attractive nature and subsequent chaining seen in results follows from the sign of the Classius - Mosatti factor.

This particular example was used to highlight *orthogonal* chaining, where chains are not formed in the traditional North-South-North-South stacking sequence of particles strongly

magnetized by an external field (or aligning due to remnant magnetization), but instead along an induced electrically polarized axis where charge distribution develops along the particles' semi-major axes. Electrics Fields of similar strength and electric and magnetic field coupling have been used experimentally by the authors to produce varying microarchitectures systems of barium hexaferrite particles in a heat curing Down Corning Sylgard polymer fluid. Details may be found in [14].

The size of the individual particles, volume fraction of particles in the composite, magnetic field strength, and electric field strength are used in a particle dynamic simulation developed in [28]. Details of the simulation methods are given in Section 2 and can be found in more detail in [24]. Results of simulations show that processing can influence micro-architecture, see Figure 1. With no external field, Figure 1a, particles form chains by stacking particles along their remnant magnetic axes, which is normal to the hexagonal plate of the actual particle and therefore lie along the semi-minor axes in simulations. In this instance there is no external field to macroscopically align the particles, therefore there is no long-range order observed. In Figure 1b, with external only an electric field applied, the particles align long their induced electrically polarized axes, which lie along a semi-major axes. Also note that the magnetic axes now show no long range order.

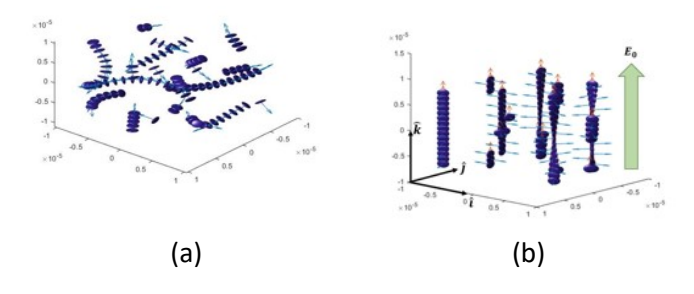


**Figure 1**: Representative simulation results of (a) no external field applied and (b) electric field only. The zero field case shows chaining due to particle remanence but no long range order while electric field case shows alignment with the external field. Blue arrows denote magnetic easy axis and red arrows induced electric dipole axis.

In the dynamics simulation, particles were modeled as barium hexaferrite, a magnetically orthotropic material with a plate like shape. The particles are 0.5  $\mu$ m along 2 of the semi axes and have an aspect ratio of 3.33 with a modulus of 152 GPa and permittivity of  $10\epsilon_0$ . The matrix material used has a modulus of 72kPa and a permittivity of  $2\epsilon_0$ . The fluid is assumed to have relative permeability of one and a viscosity of 3.5 Pa·s.

Due to the applied field, particle-particle interactions, and dielectrophoresis, the particles begin to align in chains as shown in Figure 1. The direction and orientation of each of these particles can then be used to generate a solid model geometry for a finite element analysis (FEA).

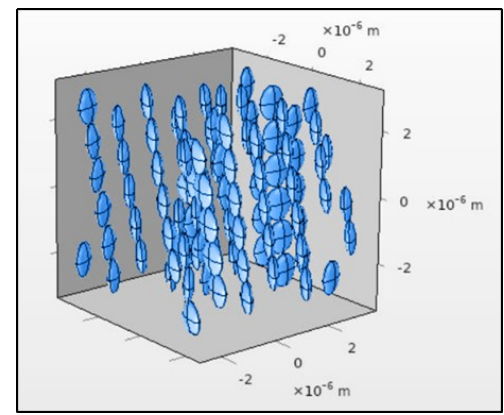


**Figure 2.** Solid model of simulations of microscale architecture of particles aligning in an electric field oriented vertically.

The centers of the particles and their orientation, generated by the processing simulations, are used in COMSOL to create a representative volume element (RVE), for which various material properties and test cases can be applied. In this work the mechanical properties of a composite were tested and compared to classical effective medium theory, specifically the Mori-Tanaka and Halpin-Tsai models. In order to populate an elasticity matrix, three normal stress and three shear stress cases were applied individually to produce a total of 6 load cases, which assumes an orthotropic symmetry to the composite.

Proscribed displacements on cubic RVE boundaries were used to generate desired macroscopic strains  $\epsilon_{i,j}$ . To prevent rigid body translation and rotation, appropriate boundary conditions were selected for each specific load case, an example of which is shown in Figure 3. In Figure 3, a positive z-displacement on the positive z-face is shown. This z-face, z-displacement combination would produce  $\epsilon_{zz}$ . The limited restrictions on motion of the negative z-face to remain the x-y plane allows free expansion in this plane, while the limits on motion along the y and z axes in the x and y planes, respectively, prevent translation in the x-y plane and rotation about any axis. Similar boundary conditions representing a cube with free faces allowed to expand freely while constraining rigid body rotation and translation were applied for all six load cases.

A surface averaged stress is calculated from the finite element analysis of the loading – boundary condition combinations, which with the known applied strain, can be used to calculate the diagonal components of the compliance matrix. Each load case isolates a given stress and strain pair, such that the diagonal entry corresponding to the given set can be expressed as

$$D_{i,i} = \frac{\varepsilon_{i,i}}{\sigma_{i,i}} \tag{3}$$

where D is the component of the compliance matrix, i is the load case number,  $\varepsilon$  is the strain, and  $\sigma$  is the stress component.

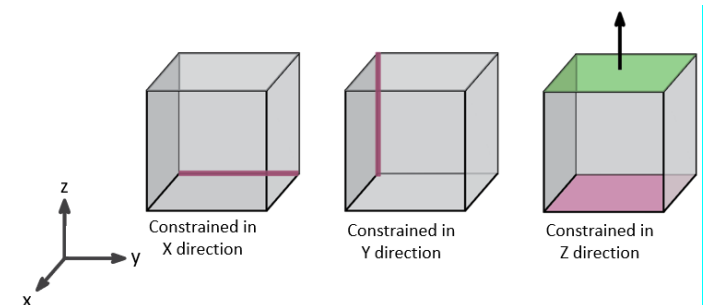


**Figure 3.** Boundary condition example for fixed displacement ε<sub>3,3</sub> where the red highlighted edges\faces had a prescribed displacement of 0m and the green highlighted face had a non-zero prescribed displacement in the indicated direction.

The full compliance matrix for an orthotropic material is

$$\begin{bmatrix} \varepsilon_{11} \\ \varepsilon_{22} \\ \varepsilon_{33} \\ \varepsilon_{12} \\ \varepsilon_{23} \end{bmatrix} = \begin{bmatrix} \frac{1}{E_1} & -\frac{\nu_{12}}{E_2} & -\frac{\nu_{13}}{E_3} \\ -\frac{\nu_{12}}{E_1} & \frac{1}{E_2} & -\frac{\nu_{23}}{E_3} \\ -\frac{\nu_{13}}{E_1} & -\frac{\nu_{23}}{E_2} & \frac{1}{E_3} \\ -\frac{\nu_{13}}{E_1} & -\frac{\nu_{23}}{E_2} & \frac{1}{E_3} \\ & & & & & \frac{1}{2G_{12}} & \frac{1}{2G_{13}} \\ \end{bmatrix} \begin{bmatrix} \sigma_{11} \\ \sigma_{22} \\ \sigma_{33} \\ \sigma_{12} \\ \sigma_{13} \\ \sigma_{23} \end{bmatrix}$$

where E is Young's modulus, G is the shear modulus and v is Poisson's ratio. These calculations are repeated for each load case to populate the diagonals. Poisson's ratio is calculated using the relationship between the known strain and one of the remaining directions' calculated values

$$\mathbf{v}_{ij} = -\frac{\varepsilon_{jj}}{\varepsilon_{ii}} \tag{14}$$

In order to determine the appropriate size of the RVE, convergence was studied for the given volume fraction as particle count is increased. Similar to Pahlavanpour et al. [20], the difference of a physical property from simulation to the expected value found using effective medium theory was considered when determining if the model is sufficiently large. In this work the compliance entries were used to determine convergence.

# 4. RESULTS AND DISCUSSION

A representative finite element solution of a solid model of a composite system is shown in Figure 4. The particles are aligned in chains as a result of the applied electric field processing. The field used in the simulations was set arbitrarily

high to induce a high degree of alignment. Due to dielectrophoresis, interaction between particles as wellas the external field, the particles themselves align edge to edge across their semi-major axes. This alignment of the particles is an artifact of the external field polarizing particles along their semi-major axis.

The representative volume shown, as well as those of other simulations conducted for this work, were subjected to the six load cases described previously. Figure four's color coding shows monotonic increase in elastic strain across the RVE with respect to the direction of the applied strain in the vertical direction as expected.

In order to determine the convergence of the system, 10% volume fraction was used and simulated for several model sizes, indicated by the particle count of the system. For this study particles formed chains in the Z(vertical) direction as a result of an applied electric field. The results for Young's modulus in the X, Y, and Z directions are shown in Figure 5, along with values for traditional effective medium models. Results are shown for a single case.

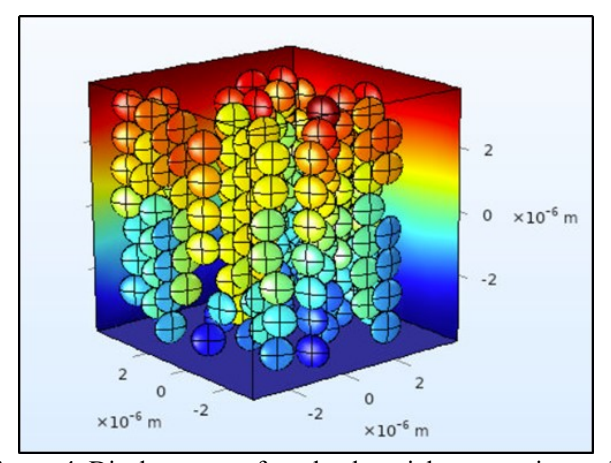


**Figure 4.** Displacement of a solved particle composite model with 10% volume fraction particle content under electric field alignment

It can be argued from Figure 5, that the modulus in the z direction, in which the particles have aligned to form chains, converges around 550 particles, with a good fit to the Mori-Tanaka model. Similarly, the x and y directions which are transverse to the chains, converge well to the Halpin-Tsai model bounds. The difference in values between x and y directions seen in the graph, is possibly a result of the aspect ratio of the ellipsoidal particles as they align in the same orientation, which can be seen in Figure 2.

The difference in modulus between the 3 directions shows the impact that not only the structures formed but the alignment within the structures which is further demonstrated in Figure 6 where a comparison of an aligned and a unaligned sample can

be seen. The compliances  $D_{11}$ ,  $D_{22}$ , and  $D_{33}$  are relatively uniform for the unaligned case, while  $D_{33}$  is reduced for the aligned case. Reduction in  $D_{33}$  with alignment is expected given the reinforcement in that direction. Though a reasonable fit to a given effective medium theory was found for each direction, no one model matched all three directions.

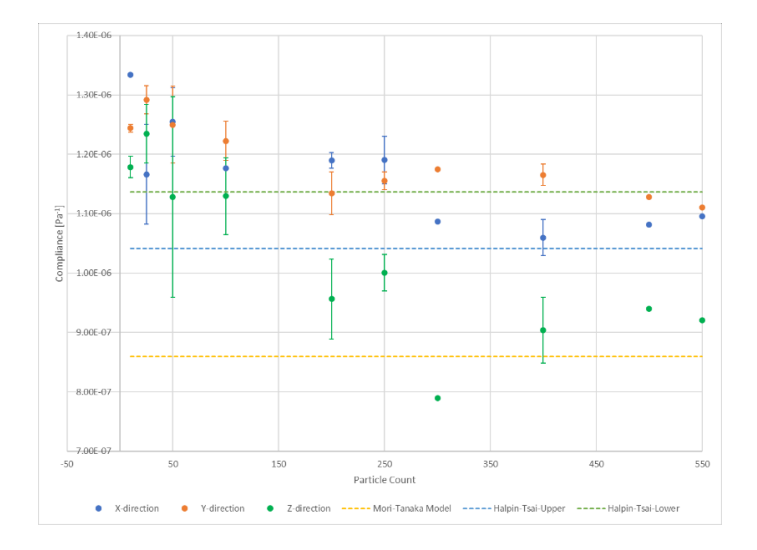


**Figure 5.** Results for simulations of modulus for various particle counts at 10% volume fraction in the 3 normal directions, x, y, and z plotted with reference lines for the Mori-Tanaka model and the Halpin-Tsai model in the upper and lower bounds. (data is shown for 5 runs at each point except 200,500, and 550 that were solved for 1 or 2 runs only)

It is important to note that simulations utilizing too few particles are inaccurate and unstable, as can be seen in the 10-50 particle range of Figure 5, demonstrating the need to solve larger models.

Similar to the study conducted by Pahlavanpour et al. [20] this simulation covered a large disparity between the modulus of the matrix (720kPa) and that of the particles (152 GPa). Moreover, the Poisson's ratio of the two materials are equally dissimilar, with that of the particles at 0.3 and that of the matrix approximated at 0.49

#### 5. CONCLUSION

The microscale structures formed by particles of a colloidal suspension of ferromagnetic particles as a result of applied electric and/or magnetic fields alter the effective material properties of the composite. It was shown that the orientation and alignment of the particles impact the compliances of the composite given the shift from isotropic to anisotropic results with the application of a field in Figure 6. Moreover, each direction agrees well with appropriate effective medium theories, supporting validation of the model and validation of the minimum size of the RVE. In future work, this modeling

framework can be used to explore not only increasing volume fractions but also various processing parameters, which result in microstructures that extends past the assumptions of effective medium theory. Future experimental validation is also an important next step.

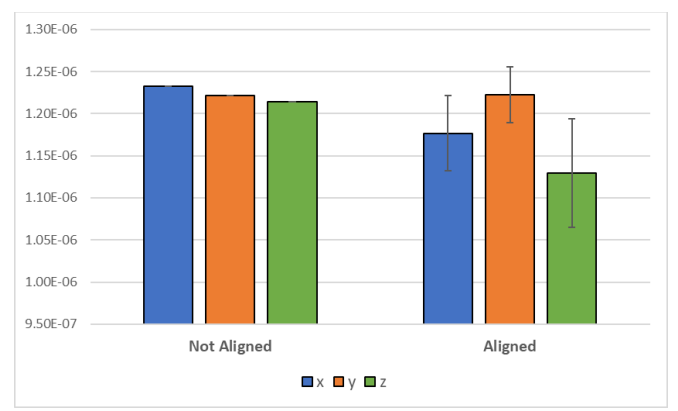


**Figure 6.** Comparison of compliance of aligned particles as a result of an applied field and non-aligned particles not subject to an applied field for 100 particles with 10% volume fraction, error bars showing standard deviation of 5 runs for the aligned case.

#### **ACKNOWLEDGEMENTS**

The authors would like to acknowledge the generous support of the National Science Foundation through NSF - CMMI-176218. Any opinions, findings, and conclusions or recommendations expressed in this material are those of the author(s) and do not necessarily reflect the views of the National Science Foundation.

# **REFERENCES**

- [1] Y. Benveniste, "A New Approach to th Application of Mori-Tanaka's Theory in Composite Materials," *Mechanics of Materials*, vol. 6, no. 2, 1987..
- [2] D. A. Van Den Ende, S. E. Van Kempen, X. Wu, W. A. Groen, C. A. Randall, and S. Van Der Zwaag, "Dielectrophoretically structured piezoelectric composites with high aspect ratio piezoelectric particles inclusions," J. Appl. Phys., vol. 111, no. 12, 2012, doi: 10.1063/1.4729814.
- [3] S. P. Gurrum, J. H. Zhao, and D. R. Edwards, "Inclusion interaction and effective material properties in a particlefilled composite material system," *J. Mater. Sci.*, vol. 46, no. 1, pp. 101–107, 2011, doi: 10.1007/s10853-010-4844-2.
- [4] S. Jin, T. N. Tiefel, and R. Wolfe, "Directionally-conductive, optically-transparent composites by magnetic alignment," *IEEE Trans. Magn.*, vol. 28, no. 5, pp. 2211–2213, Sep. 1992, doi: 10.1109/20.179446.
- [5] Z. Varga, G. Filipcsei, and M. Zrínyi, "Magnetic field sensitive functional elastomers with tuneable elastic

- modulus," *Polymer*, vol. 47, no. 1, pp. 227–233, Jan. 2006, doi: 10.1016/j.polymer.2005.10.139.
- [6] J. S. Leng, W. M. Huang, X. Lan, Y. J. Liu, and S. Y. Du, "Significantly reducing electrical resistivity by forming conductive Ni chains in a polyurethane shape-memory polymer/carbon-black composite," *Appl. Phys. Lett.*, vol. 92, no. 20, p. 204101, May 2008, doi: 10.1063/1.2931049.
- [7] C. Breznak and P. von Lockette, "Particle orientation and bulk properties of magnetoactive elastomers fabricated with aligned barium hexaferrite," *J. Mater. Res.*, vol. 34, no. 6, pp. 972–981, Mar. 2019, doi: 10.1557/jmr.2018.496.
- [8] D. S. Jones, *The Theory of Electromagnetism*. Pergamon Press, 1964.
- [9] S. Odenbach, Ed., Colloidal Magnetic Fluids: Basics, Development and Application of Ferrofluids, vol. 763. Berlin, Heidelberg: Springer Berlin Heidelberg, 2009.
- [10] J. M. M. Linke and S. Odenbach, "Anisotropy of the magnetoviscous effect in a ferrofluid with weakly interacting magnetite nanoparticles," *J. Phys. Condens. Matter J Phys Condens Matter*, vol. 27, p. 7, 2015, doi: 10.1088/0953-8984/27/17/176001.
- [11] L. M. Pop and S. Odenbach, "Capillary viscosimetry on ferrofluids," 2008, doi: 10.1088/0953-8984/20/20/204139.
- [12] O. D. Velev and K. H. Bhatt, "On-chip micromanipulation and assembly of colloidal particles by electric fields," *Soft Matter*, vol. 2, no. 9, pp. 738–750, 2006, doi: 10.1039/b605052b.
- [13] B. Bharti, F. Kogler, C. K. Hall, S. H. L. Klapp, and O. D. Velev, "Multidirectional colloidal assembly in concurrent electric and magnetic fields," *Soft Matter*, vol. 12, no. 37, pp. 7747–7758, 2016, doi: 10.1039/c6sm01475e.
- [14] M. Al Masud, A. Erol, C. Edson, Z. Ounaies, and P. VonLockette, "Towards complex microarchitectural nanocomposites using non-uniform multi-field processing," no. March 2019, p. 15, 2019, doi: 10.1117/12.2515259.
- [15] S. Gangwal, O. J. Cayre, M. Z. Bazant, and O. D. Velev, "Induced-Charge Electrophoresis of Metallodielectric Particles," 2008, doi: 10.1103/PhysRevLett.100.058302.
- [16] B. Bharti and O. D. Velev, "Multidirectional, Multicomponent Electric Field Driven Assembly of Complex Colloidal Chains," Z. Phys. Chem., vol. 229, no. 7–8, pp. 1075–1088, 2015, doi: 10.1515/zpch-2014-0543.
- [17] O. D. Velev, S. Gangwal, and D. N. Petsev, "Particle-localized AC and DC manipulation and electrokinetics," Annu. Rep. Prog. Chem. - Sect. C, vol. 105, pp. 213–246, 2009, doi: 10.1039/b803015b.
- [18] X. Zhao, Y. Wu, Z. Fan, and F. Li, "Three-dimensional simulations of the complex dielectric properties of random composites by finite element method," *J. Appl. Phys.*, vol. 95, no. 12, pp. 8110–8117, 2004, doi: 10.1063/1.1712017.
- [19] J. Segurado and J. Llorca, "A numerical approximation to the elastic properties of sphere-reinforced composites," 2002. [Online]. Available: www.elsevier.com/locate/jmps.

- [20] M. Pahlavanpour, H. Moussaddy, E. Ghossein, P. Hubert, and M. Lévesque, "Prediction of elastic properties in polymer–clay nanocomposites: Analytical homogenization methods and 3D finite element modeling," *Comput. Mater. Sci.*, vol. 79, pp. 206–215, Nov. 2013, doi: 10.1016/j.commatsci.2013.06.029.
- [21] M. Kallio, T. Lindroos, S. Aalto, E. Järvinen, T. Kärnä, and T. Meinander, "Dynamic compression testing of a tunable spring element consisting of a magnetorheological elastomer," *Smart Mater. Struct.*, vol. 16, no. 2, pp. 506–514, Apr. 2007, doi: 10.1088/0964-1726/16/2/032.
- [22] H. Deng, X. Gong, and L. Wang, "Development of an adaptive tuned vibration absorber with magnetorheological elastomer," *Smart Mater. Struct.*, vol. 15, no. 5, pp. N111–N116, Oct. 2006, doi: 10.1088/0964-1726/15/5/N02.
- [23] G. Y. Zhou and Q. Wang, "Magnetorheological elastomer-based smart sandwich beams with nonconductive skins," *Smart Mater. Struct.*, vol. 14, no. 5, pp. 1001–1009, Oct. 2005, doi: 10.1088/0964-1726/14/5/038.
- [24] M.A. Rodriguez, and P. von Lockette,. "PDF Evolution of Texture in the Fabrication of Magneto-Active Elastomers." Proceedings of the ASME 2017 Conference on Smart Materials, Adaptive Structures and Intelligent Systems. Volume 1: Development and Characterization of Multifunctional Materials; Mechanics and Behavior of Active Materials; Bioinspired Smart Materials and Systems; Energy Harvesting; Emerging Technologies. Snowbird, Utah, USA. September 18–20, 2017. V001T01A008. ASME.
- [25] M. Mohebi, N. Jamasbi, and J. Liu, "Simulation of the formation of nonequilibrium structures in magnetorheological fluids subject to an external magnetic field," *Phys. Rev. E*, vol. 54, no. 5, pp. 5407–5413, Nov. 1996, doi: 10.1103/PhysRevE.54.5407.
- [26] H. V. Ly, F. Reitich, M. R. Jolly, H. T. Banks, and K. Ito, "Simulations of Particle Dynamics in Magnetorheological Fluids | Elsevier Enhanced Reader," *Journal of Computational Physics*, vol. 155, no. 1, pp. 160–1777, Oct. 1999, doi: https://doi.org/10.1006/jcph.1999.6335.
- [27] R. E. Rosenzweig, Ferrohydrodynamics. Mineola NY: Dover, 1997.
- [28] Erol, Anil, "studies of Dipole-Driven active Materials: Multifield Processing Simulations, Microstructure-Based Constitutive Modeling, and Macroscopic Compisite Optimization," The Pennsylvania State University, 2019.